hydroxamic acid ligand does not significantly affect the chelation reactivity of the third uncoordinated hydroxamate group. Hence, we propose that the mechanism already described for the formation and hydrolysis of the bidentate-coordinated ferrioxamine B complex[8,9] is probably operative in the interconversion of the fully coordinated binuclear diferrioxamine B to the mononuclear tetradentate-linked ferrioxamine B complex.

The hydrolysis of the diferrioxamine B complex proceeds by two parallel acid-dependent and acid-independent pathways exhibiting rate constants of magnitude similar to those of the hydrolysis of the bidentate-bonded ferrioxamine B. These observations indicate a release, during hydrolysis, of ferric ion bound to only one hydroxamate group, since to propose otherwise, one would expect one pathway and the rate constant corresponding to the hydrolysis rate constant either of fully bound ferrioxamine B (k_{-3} = 16.4 M^{-1} s^{-1}) or of tetradentate-linked ferrioxamine B (k_{-2} = 2 M^{-1} s^{-1}).

The obtained data indicate that one hydroxamic acid group of the trihydroxamic acid also exhibits a high specificity for chelating iron(III) when the remaining hydroxamate functions are coordinated to the ferric ion. The spherically symmetric +3 oxidation state is the most important feature of ferric ions related to the the high biological selectivity of hydroxamic acid for high-spin iron(III) since the other biologically important metal ions are mainly in the +2 oxidation state.[7,20] In addition Monzyk and Crumbliss have shown in their excellent studies[7] that the enhanced thermodynamic and kinetic stability of (hydroxamato)iron(III) complexes is due to the delocalization of the N atom lone pair into the carbonyl functionality. This delocalization is strongly influenced by the electron donor ability of the organic substituents, such as alkyl, bound to the N atom.

The similarity of steps 1 and 4 of Scheme I suggests that the coordination of two hydroxamate groups of desferrioxamine B to iron(III) does not influence the electronic properties of the free hydroxamate functionality. This is a reasonable assumption since the hydroxamate groups are separated in desferrioxamine B by nine atoms. For the same reason the steric factors probably do not play an important role in the formation of the 14-membered ring when two or three hydroxamate groups of desferrioxamine B are coordinated to ferric ion.

Acknowledgment. The authors appreciate financial support from the Croatian Council for Research (SIZ II) and the National Institute of Health (Grant No. 02-100-N).

Registry No. Fe, 7439-89-6; ferrioxamine B, 14836-73-8; desferrioxamine B, 70-51-9.

(20) Sillen, L. G.; Martell, A. E. *Spec. Publ.—Chem. Soc.* **1964**, *No. 17*; **1971**; *No. 25*. Martell, A. E.; Smith, R. M. "Critical Stability Constants"; Plenum Press: New York, 1977; Vol. 3.

Contribution from the Department of Chemistry, The University of Texas at Austin, Austin, Texas 78712

Electrochemical and Spectrophotometric Studies of Iron Complexes with a Pentaaza Macrocyclic Ligand

YIH-WEN D. CHEN and ALLEN J. BARD*

Received September 23, 1983

Aqueous solutions of complexes of iron(III) and iron(II) and the macrocyclic ligand 2,13-dimethyl-3,6,9,12,18-pentaazabicyclo[12.3.1]octadeca-1(18),2,12,14,16-pentaene (B) were investigated by voltammetry, chronocoulometry, and controlled-potential coulometry. Standard potentials for redox reactions involving species in this system, which include FeB^{3+}, $FeB(OH)^{2+}$, and FeB^{2+}, as well as binuclear species such as $(FeB)_2O^{4+}$, were obtained, and reactions involving decomposition of these at different pHs were investigated. Spectrophotometric measurements were also employed in the elucidation of the chemistry of this system.

Introduction

The desire to find highly water soluble and stable redox couples based on inexpensive materials for use as components in photoelectrochemical cells and redox storage batteries has led us to investigate bipyridine and phenanthroline complexes of iron and cobalt.[1,2] We have also investigated macrocyclic compounds as ligands with these metals in an attempt to determine the factors that govern the redox potentials, heterogeneous kinetics, and stabilities of these complexes. We report here results of studies of iron(II) and iron(III) complexes with the pentaaza macrocyclic ligand 2,13-dimethyl-3,6,9,12,18-pentaazabicyclo[12.3.1]octadeca-1-(18),2,12,14,16-pentaene (B). This ligand, which, in the presence of axial coordinating species, forms a seven-coordinate complex with iron, was first synthesized and characterized by

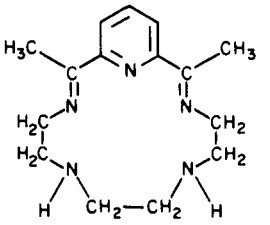

B

Busch and co-workers.[3-5] These species in solution probably involve water molecules in the axial positions and will be denoted as FeB^{3+} and FeB^{2+}. The solution chemistry is com-

(1) Chen, Y.-W. D.; Santhanam, K. S. V.; Bard, A. J. *J. Electrochem. Soc.* **1981**, *128*, 1460.
(2) Chen, Y.-W. D.; Santhanam, K. S. V.; Bard, A. J. *J. Electrochem. Soc.* **1982**, *129*, 61.
(3) Curry, J. D.; Busch, D. H. *J. Am. Chem. Soc.* **1964**, *86*, 593.
(4) Nelson, S. M.; Busch, D. H. *Inorg. Chem.* **1969**, *8*, 1859.
(5) Nelson, S. M.; Bryan, P.; Busch, D. H. *J. Chem. Soc., Chem. Commun.* **1966**, 641.

0020-1669/84/1323-2175$01.50/0

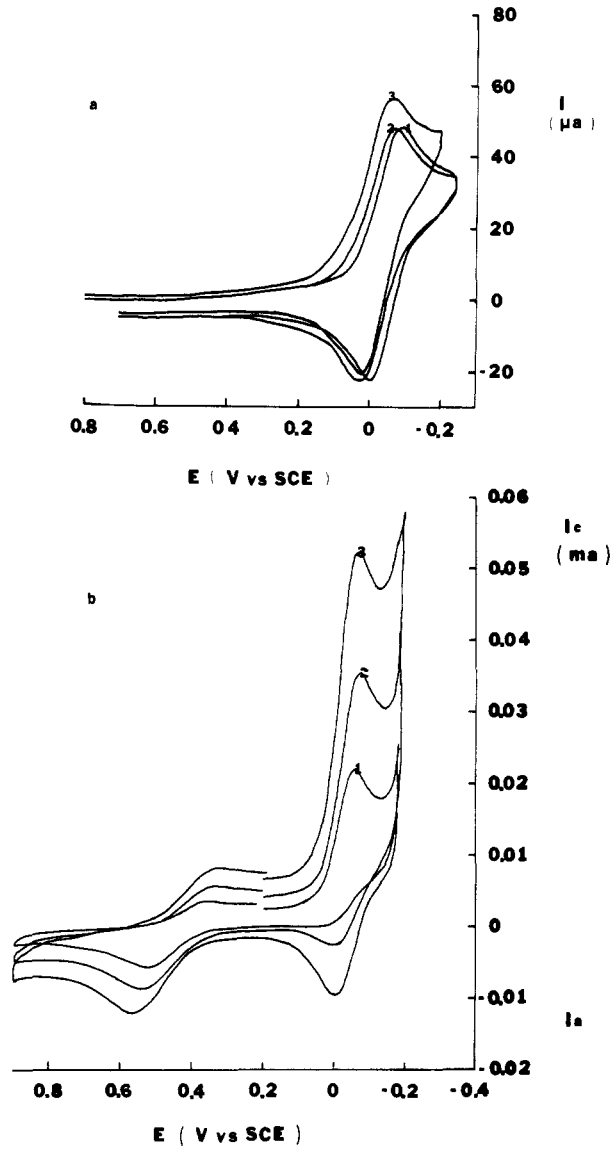

Figure 1. Cyclic voltammetry of FeB^{3+} at a Pt electrode: (a) 4 mM FeB^{3+} in 0.5 M H_2SO_4, scan rate 100 mV/s; (b) 10 mM FeB^{3+} in 4.5 M H_2SO_4, scan rates (1) 20, (2) 50, and (3) 100 mV/s.

plicated by the formation of binuclear species with the central irons connected by an oxygen bridge

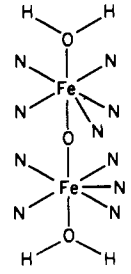

$(H_2O)BFe\text{-}O\text{-}FeB(H_2O)^{4+}$

at higher pHs. The structure of such a complex of iron(II) and B has been examined by X-ray crystallography[6] and infrared, magnetic, and conductivity measurements;[5] similar binuclear oxygen-bridged species of bidentate and tetraaza macrocyclic ligands have also been studied.[7-11] The iron(III)

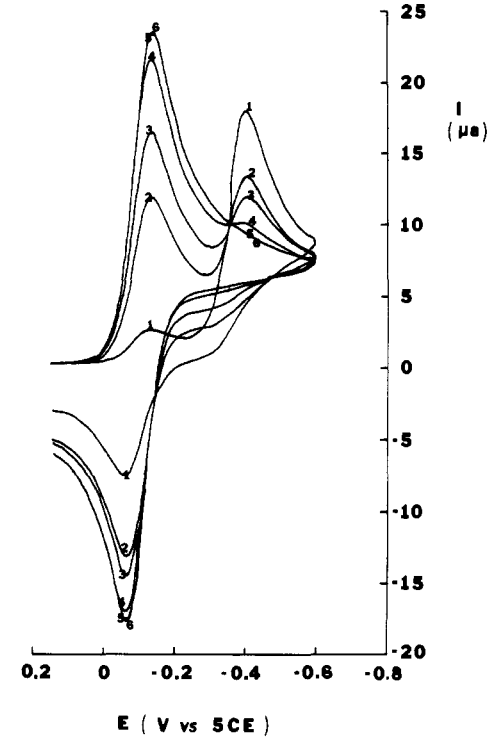

Figure 2. Cyclic voltammetry of 2.5 mM $(FeB)_2O^{4+}$ in 2.5 M 1:1 acetic acid/acetate buffer, pH 4.7, at a hanging-Hg-drop electrode at 200 mV/s obtained (1) 0, (2) 18, (3) 36, (4) 86, (5) 166, and (6) 206 min after addition of solid perchlorate salt to buffer.

species will be denoted as $(FeB)_2O^{4+}$.

Experimental Section

Complete experimental details including sources of reagents, apparatus, and procedures are available.[12] Electrochemical and spectrophotometric measurements followed usual practice.

The macrocyclic 3+ ion complexes $FeB(OH)(ClO_4)_2$ and $(FeB)_2O(ClO_4)_4 \cdot H_2O$ were prepared and characterized by the procedures of Busch et al.[3,4] At least 1 day elapsed between the preparation of acidic aqueous solutions of the iron(III) complex and the electrochemical measurements to allow the system to equilibrate. However, the aqueous basic solutions of the iron(III) complex were prepared and used immediately to avoid decomposition of the iron(III) complex in the strongly basic media.

Controlled-potential electrolysis employed a large-area (6.5 cm^2) graphite-sheet electrode (Ultra Carbon, Sherman, TX) with nitrogen deaeration. All potentials were measured with respect to an aqueous saturated calomel electrode (SCE). An H-cell with a porous sintered-glass disk separating the two compartments was used in coulometric investigations. For cyclic voltammetric investigations, a single-compartment cell with a solution capacity of 5 mL was employed, with either a platinum-disk (0.114 cm^2), graphite-rod (0.20 cm^2), or hanging-mercury-drop (A = 0.010 25 cm^2) working electrode. The platinum electrode was polished with 0.3-μm and then 0.05-μm alumina before each measurement.

Results

Cyclic Voltammetry. The number and nature of the cyclic voltammetric (CV) waves depended upon solution pH and experimental conditions. A strongly acidic solution (e.g., 0.5 M H_2SO_4) of the iron(III) complex at scan rates (v) above 0.1 V/s produces a single pair of waves with E_{pc} at −0.1 V vs. SCE (Figure 1a). This is ascribed to the reaction

$$FeB^{3+} + e^- \rightleftarrows FeB^{2+} \quad (1)$$

(6) Fleischer, E.; Hawkinson, S. *J. Am. Chem. Soc.* **1967**, *89*, 720.
(7) Murray, K. S. *Coord. Chem. Rev.* **1974**, *12*, 1.
(8) Anderegg, G. *Helv. Chim. Acta* **1982**, *45*, 1643.
(9) Reiff, W. M.; Baker, W. A., Jr.; Erickson, N. E. *J. Am. Chem. Soc.* **1968**, *90*, 4794.
(10) Reiff, W. M.; Long, G. J.; Baker, W. A., Jr. **1968**, *90*, 6347.
(11) Parker, O. J.; Espenson, J. H. *Inorg. Chem.* **1969**, *8*, 185.
(12) Chen, Y.-W. D. Ph.D. Dissertation, The University of Texas at Austin, 1982.

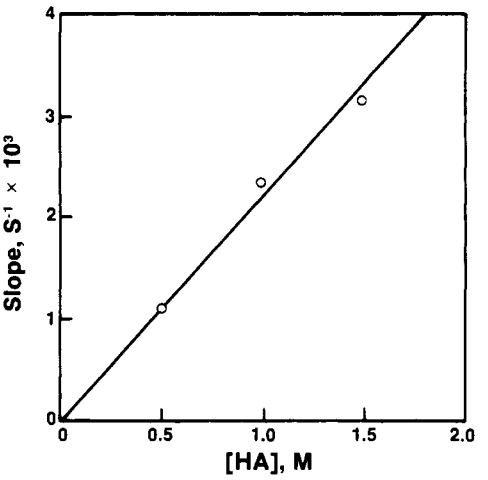

Figure 3. Slopes of ln $[i_{pc}(t)]$ vs. t plots vs. total molar concentration of buffer components (1:1 cyanoacetic acid/cyanoacetate pH 2.45).

The FeB^{3+} species is very stable under these conditions, since the CV behavior was virtually unchanged for iron(III)–B for solutions at least 1 year old. In more acidic solutions (4–5 M), the FeB^{2+} species is not very stable with respect to dissociation to Fe^{2+} and free ligand (eq 2). This is shown by

$$FeB^{2+} \rightleftharpoons Fe^{2+} + B \qquad (2)$$

CV scans of FeB^{3+} solutions at lower scan rates (Figure 1b) where the reverse anodic wave at −0.0 V decreases and at $v < 0.02$ V/s where it disappears, and a pair of waves for the $Fe^{3+/2+}$ aqueous complexes arises at more positive potentials.

When the binuclear iron(III) complex $(FeB)_2O^{4+}$ (in the form of the perchlorate salt) is added to an acidic aqueous solution (pH <6), the solution is initially brown but turns yellow with time. Initially cyclic voltammetry shows a wave at ~−0.4 V, but with time this wave height decreases and the pair of waves of the $FeB^{3+/2+}$ couple at −0.1 V grows in; see, for example, the results at pH 4.7 in Figure 2. The rate of color change and growing in of the mononuclear complex waves was faster at lower pH. Thus, reaction 3 occurs, and

$$(FeB)_2O^{4+} + 2H^+ \rightarrow 2FeB^{3+} + H_2O \qquad (3)$$

at these pHs the binuclear complex is completely converted to the mononuclear species. The rate of the decomposition reaction (3) could be monitored by determining the formation of FeB^{3+} as a function of time, t, from the growth of the peak current of the cathodic wave at −0.1 V, $i_{pc}(t)$. Plots of ln $[i_{pc}(t)]$ vs. t were linear for pH 2.45 1:1 cyanoacetic acid (HCNA)/cyanoacetate buffers at total component concentrations of 1–3 M. The rate of decomposition at this pH was proportional to the total buffer concentration, since a plot of the slopes of the log $[i_{pc}(t)]$ vs. t lines against total buffer concentration was linear with a zero intercept (Figure 3). Thus, the rate-determining step in reaction 3 is probably attack of the binuclear complex by the undissociated acid, HCNA; the pseudo-first-order rate constant for this pH was 2.0×10^{-3} M^{-1} s^{-1} (25 °C).

Breakup of the binuclear iron(III) species also occurs in strongly alkaline solution. When the $(FeB)_2O^{4+}$ species is dissolved in 1 M NaOH, the solution is initially colorless and shows a CV wave at −0.85 V (Figure 4). After several hours the solution becomes turbid with eventual formation of a brown precipitate, and the CV waves decrease in height. The brown precipitate when dissolved in 0.5 M H_2SO_4 shows only the CV waves of the uncomplexed $Fe^{3+/2+}$ couple (at 0.5 V), suggesting that dissociation of the complex occurs with formation of hydrous ferric oxide (represented in eq 4 by Fe_2O_3). The

$$(FeB)_2O^{4+} + 4OH^- \rightarrow Fe_2O_3 + 2H_2O + 2B \qquad (4)$$

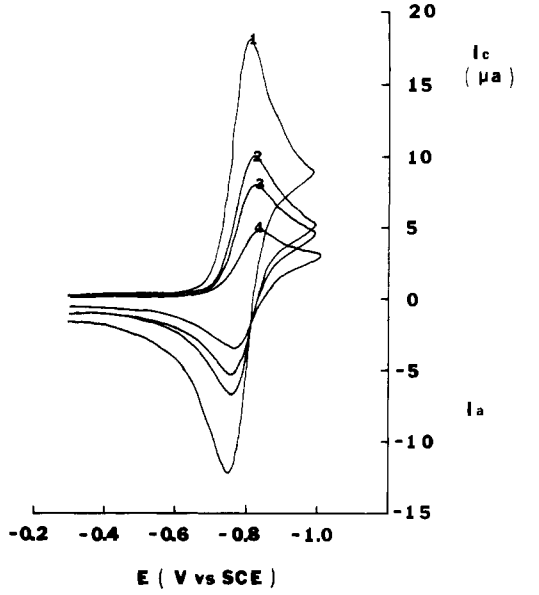

Figure 4. Cyclic voltammetry of 2.5 mM $(FeB)_2O^{4+}$ in 1 M NaOH at a hanging-Hg-drop electrode at 100 mV/s obtained (1) 0, (2) 15, (3) 22, and (4) 42 h after solution preparation.

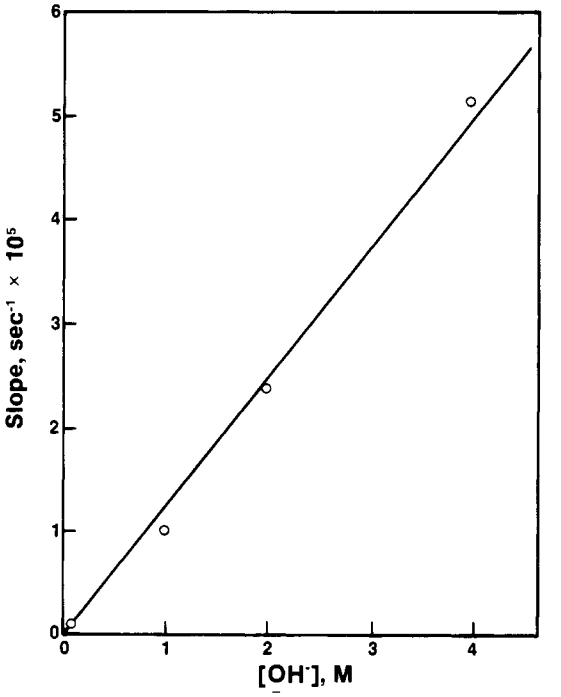

Figure 5. Slopes of ln $[i_{pc}(t)/i_{pc}(0)]$ vs. t plots vs. hydroxide ion concentration for 2.5 mM $(FeB)_2O^{4+}$ in alkaline media.

chloroform extract, when analyzed by mass spectroscopy and infrared spectrophotometry, showed the presence of the free ligand, B, and 2,6-diacetylpyridine.[12] The rate of decomposition of the binuclear iron(III) complex in alkaline solutions was monitored by the decrease in the peak cathodic current. Plots of ln $[i_{pc}(t)/i_{pc}(0)]$ vs. t were linear for 1, 2, 3.2, and 4 M NaOH solutions. A plot of the slopes of these lines vs. hydroxide concentration was linear (Figure 5), suggesting decomposition in alkaline solution followed the rate law $dC/dt = -k_2'[OH]C$, where C is the complex concentration and $k_2' = 1.2 \times 10^{-5}$ M^{-1} s^{-1} (25 °C).

The iron(III) binuclear complex was more stable in nearly neutral solutions (e.g., unbuffered 0.5 M Na_2SO_4) (Figure 6). Immediately after dissolution a well-defined reduction peak at −0.7 V is observed. On reversal, only a small anodic wave is found near these potentials, with the appearance of rather

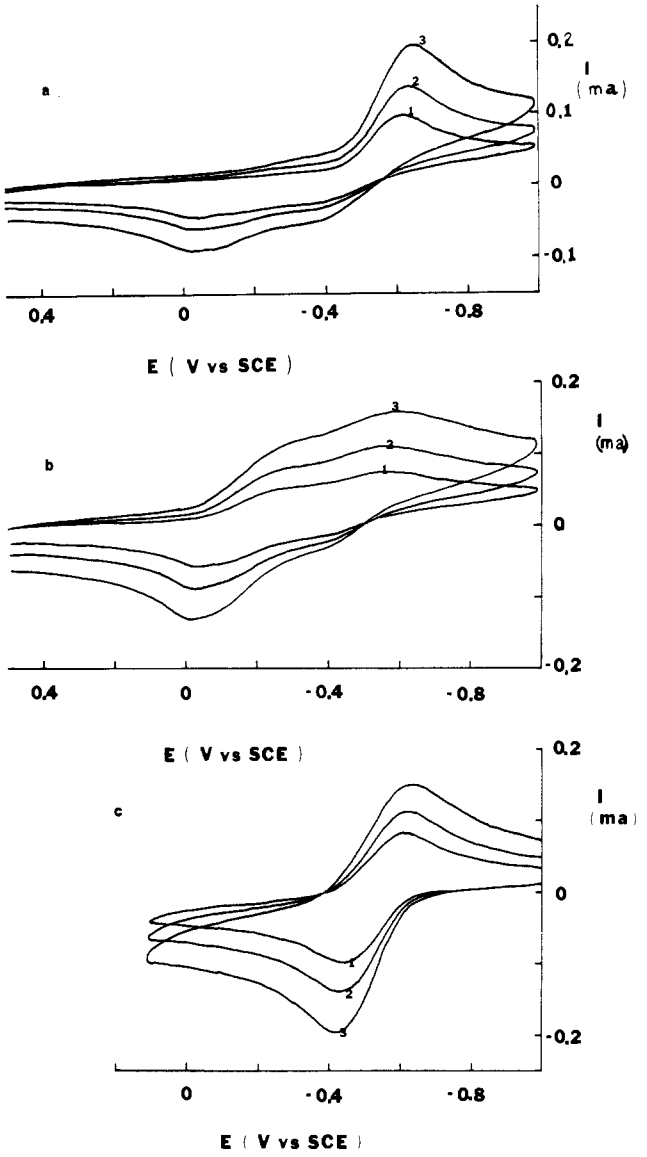

Figure 6. Cyclic voltammetry of 2.5 mM $(FeB)_2O^{4+}$ in 0.5 M Na_2SO_4 (a) just after dissolution, (b) after 1 day, and (c) after exhaustive electrolysis at −0.85 V (scan rates (1) 20, (2) 50, and (3) 100 mV/s).

broad anodic waves at more positive potentials (Figure 6a). Solutions examined several hours after preparation showed the cathodic wave greatly broadened with the anodic wave at −0.1 V more pronounced (Figure 6b).

Cyclic voltammetric curves produced by dissolving the iron(III) binuclear complex into unbuffered Na_2SO_4 and adjusting the pH to different values with strong acid and base are shown in Figure 7. The CV curve 7a was measured immediately after dissolution of the binuclear complex and is similar to that in Figure 6a. The other CV curves were measured after the pH was adjusted and the solution was allowed to equilibrate. Only one cathodic/anodic wave pair was observed at high (curves b and c) or low (curves n and o) pH, while several, often less well-defined, cathodic and anodic waves were found for pHs between 6 and 12 (curves d–m).

The CV wave pairs in most cases showed peak separations ($E_{pa} - E_{pc}$) near 60 mV, suggesting that the electrode reactions approached Nernstian behavior. In these cases, formal potentials were estimated for these reactions; these are listed in Table I and are also given in Figure 8, which will be discussed below.

Coulometric Measurements. Additional information about the nature of the redox and dissociation reactions of the iron

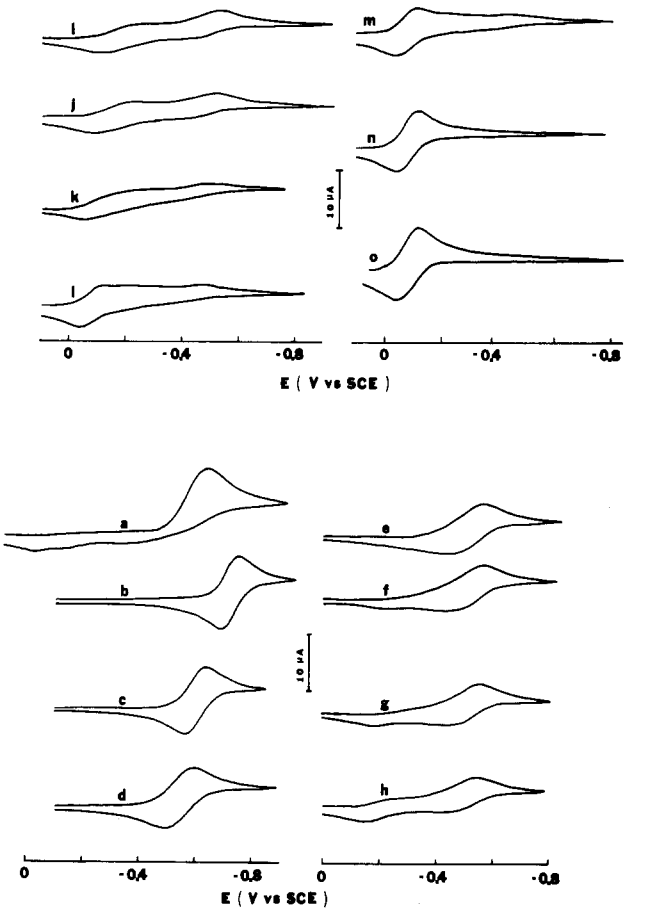

Figure 7. Cyclic voltammograms of the iron(III)–B system in 0.5 M Na_2SO_4 adjusted to pH (a) 7.33, (b) 12.96, (c) 12.02, (d) 11.32, (e) 10.57, (f) 9.92, (g) 9.50, (h) 8.83, (i) 8.25, (j) 7.74, (k) 7.00, (l) 6.53, (m) 6.25, (n) 5.45, and (o) 4.00 (iron concentration 5 mM; hanging-Hg-drop electrode; scan rate 100 mV/s).

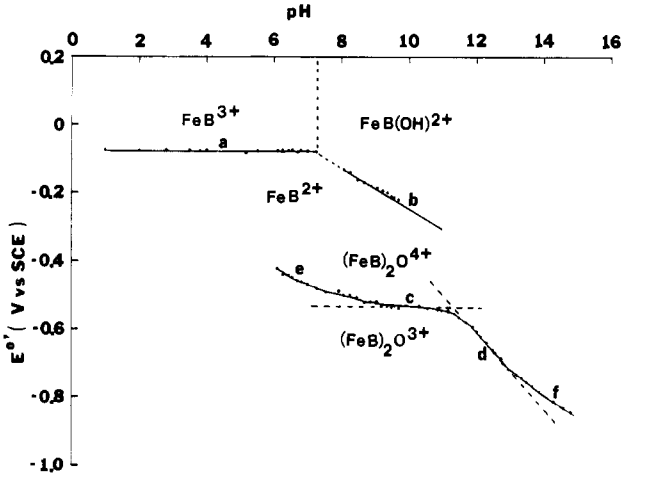

Figure 8. Estimated formal potentials of the iron–B system from cyclic voltammetry results as a function of pH.

chelate species was obtained from observations of pH changes and controlled-potential coulometry measurements. For example, when a solution of the iron(III) binuclear complex (2.5 mM) was prepared in 5 mM HCl, the pH changed from 2.3 to 2.8 after 2 days and to 3.0 after 5 days, demonstrating that dissociation of the complex is accompanied by the consumption of protons, as in eq 3. Similarly, a 5 mM $(FeB)_2O^{4+}$ solution in 10 mM HCl changed from pH 2.0 to 2.3. After equilibrium was attained, only a single CV wave, characteristic of the FeB^{3+} species, was observed. Controlled-potential electrolysis of this solution at −0.15 V vs. SCE consumed 2 faradays/mol

Table I. Formal Potentials from Cyclic Voltammetric Data for the Iron–B System[a]

pH	1st $E^{\circ\prime}$, V vs. SCE	2nd $E^{\circ\prime}$, V vs. SCE	pH	2nd $E^{\circ\prime}$, V vs. SCE
1.0	−0.075		11.17	−0.550
2.0	−0.075		11.68	−0.580
3.5	−0.075		12.02	−0.604
4.0	−0.076		12.57	−0.666
5.17	−0.081		12.96	−0.718
6.10	−0.078	−0.420	12.9	−0.71
6.72	−0.081	−0.458	13.3	−0.74
7.00	−0.078	−0.470	13.7[b]	−0.76
8.06	−0.130	−0.498	14.0[b]	−0.79
8.67	−0.170	−0.518	14.3[b]	−0.81
9.05	−0.184	−0.518	14.6[b]	−0.83
9.50	−0.210	−0.536	14.7[b]	−0.84
9.92	−0.230	−0.530		

[a] Solutions were 0.5 M Na_2SO_4 adjusted to pH by addition of NaOH or concentrated H_2SO_4, unless noted otherwise (measured at 25 °C). [b] NaOH solutions.

of original iron(III) binuclear complex (i.e., n_{app} = 2 or 1 electron/FeB^{3+}). A cyclic voltammogram after electrolysis, with an initial anodic scan, showed the same pair of waves, with essentially equal peak currents. For a 2.5 mM solution of binuclear complex in 0.5 M Na_2SO_4 (pH 7.2) (see Figure 6a) controlled-potential electrolysis at −0.85 V again showed n_{app} = 2 with the pH 11.3 after electrolysis; the cyclic voltammogram obtained is shown in Figure 6c. This is assigned to oxidation of the iron(II) binuclear complex. Oxidation of this solution at +0.35 V consumed essentially the same number of coulombs as the first electrolysis, and the pH returned to 7.2. However, the cyclic voltammogram now was the same as that in Figure 6b, showing that appreciable dissociation had occurred. Coulometric reduction of this solution at −0.85 V again consumed the same number of coulombs and produced a solution of pH 11.3; the voltammetry of this solution closely resembled that of Figure 6c.

Dissolution of the binuclear complex (2.5 mM) in 5 mM NaOH showed a change from pH 11.7 to 9.3 after several minutes. This can be ascribed to the conversion of $(FeB)_2O^{4+}$ to the hydroxylated form, $(FeB)_2O(OH)_2^{2+}$. Electrolysis of the iron(III) binuclear complex in 1 M NaOH immediately after dissolution (i.e., the colorless solution before decomposition via eq 4) at −1.0 V occurs with n_{app} = 2.0.

Heterogeneous Electron-Transfer Rate Constants. Diffusion coefficients (D) and the rate constants for the electron-transfer reactions (k^0) for the electrode reaction in eq 1 were obtained from chronocoulometric measurements monitoring charge (Q) with time for a step to a given potential.[1,2,12,13] Typical Q vs. t and Q vs. $t^{1/2}$ plots are given in Figure 9, and results are summarized in Tables II and III. The heterogeneous rate constant at a platinum electrode was a function of the electrolyte composition and was largest in 0.1 M HNO_3, 2 M KNO_3, and 0.1 M HCl/2 M KCl media. Lower values were found in sulfate and the less acidic buffer (Table II). Moreover, addition of iodide to the nitrate medium caused a decrease in k^0, while addition of Cl^- to the sulfate medium caused an increase in k^0 (Table III).

Spectrophotometric Measurements. Measurements of solution absorbance at different pHs and as a function of time generally confirmed the assignment of species and rate constants obtained from the electrochemical measurements. The FeB^{3+} complex in acidic solution is pale yellow with λ_{max} of 520–535 nm and ϵ_{max} of 1–7 M^{-1} cm^{-1} (the values depend slightly on the pH and the nature of the buffer; see Table II).

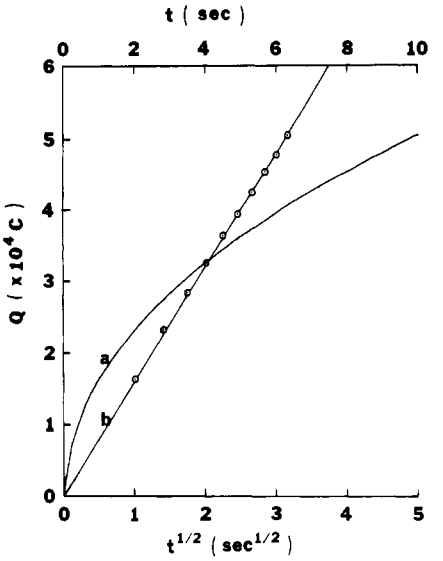

Figure 9. Typical chronocoulometric results for 5 mM FeB^{3+} in 1 M 1:1 acetic acid/acetate buffer: (a) charge vs. time; (b) charge vs. $t^{1/2}$.

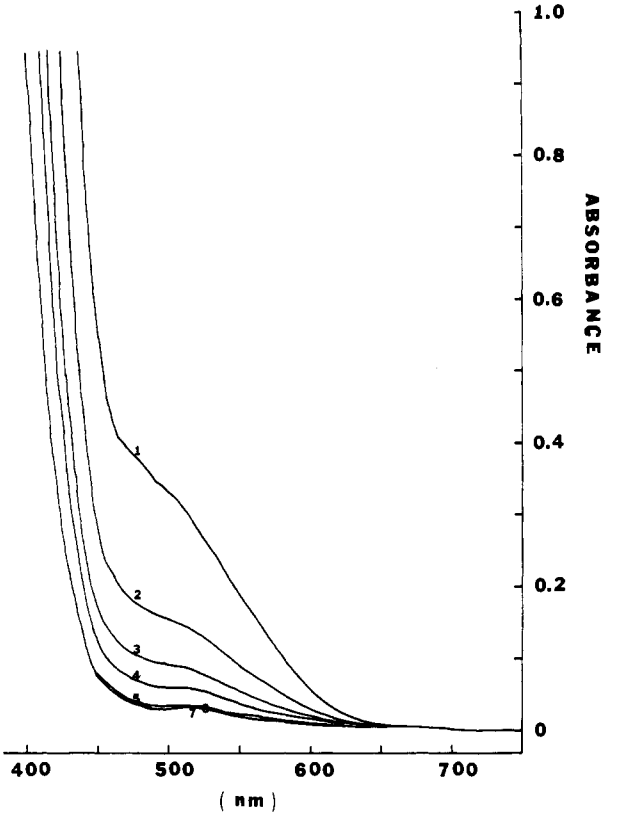

Figure 10. Absorbance curves for 2 mM $(FeB)_2O^{4+}$ added to 2.5 M 1:1 acetic acid/acetate buffer (1) 0, (2) 15, (3) 30, (4) 50, (5) 135, (6) 225, and (7) 295 min after dissolution of perchlorate salt.

When the iron(III) binuclear complex is added to an acidic solution (e.g., an acetic acid/acetate buffer) (Figure 10), the initially brownish solution, which shows a broad absorption below 650 nm, slowly turns yellow. This corresponds to the dissociation reaction, eq 3. The rate of disappearance of $(FeB)_2O^{4+}$ was obtained by monitoring the absorbance at 475 nm as a function of time, t. For example, for a 1 M 1:1 cyanoacetic acid/acetate buffer, a plot of $-\ln [(A - A_\infty)/(A_0 - A_\infty)]$ vs. t (where A, A_0, and A_∞ are the absorbances at time t, at initial time, and after equilibrium is attained, respectively) was linear, showing a pseudo-first-order reaction. The pseudo-first-order rate constant so obtained, k_2, varied linearly

(13) Bard, A. J.; Faulkner, L. R. "Electrochemical Methods: Fundamentals and Applications"; Wiley: New York, 1980; pp 199–206.
(14) Latimer, H. A.; Harris, W. E. "Chemical Analysis"; McGraw-Hill: New York, 1975; p 231.

Table II. Potentials, Heterogeneous Rate Constants, and Spectrophotometric Data for the Iron(III) Complex of B in Aqueous Solution[a]

medium	pH	$E^{\circ\prime}(3\rightarrow2)$, V vs. SCE	$k^{\circ\prime}$, cm/s	$10^6 D_0$, cm^2/s	λ_{max} nm (ϵ_{max}, M^{-1} cm^{-1})
1 M 1:1 trifluoroacetic acid	0.084	0.041	0.088	5.61	535 (3.2)
0.1 M HNO_3/2 M KNO_3	1.0	0.080	0.12	5.41	535 (2.8)
0.1 M HCl/2 M KCl	1.0	0.021	0.11	4.12	535 (3.2)
0.05 M H_2SO_4/0.5 M Na_2SO_4	1.92	−0.071	0.012	4.38	525 (2.8)
1 M 1:1 cyanoacetic acid	2.45	−0.018	0.020	4.42	525 (6.0)
1 M 1:1 tartaric acid	3.03	−0.064	0.0023	3.02	525 (6.0)
1 M 1:1 acetic acid	4.74	−0.10	0.024[b]	4.55	525 (4.6)
1 M 1:1 propionic acid	4.90	−0.10	0.035	4.15	525 (3.6)
1 M 1:1 malonic acid	4.87	−0.14	0.013	2.95	520 (1.2)
1 M 1:1 adipic acid	5.16	−0.15	0.010	2.90	525 (6.4)
1 M 1:1 succinic acid	5.16	−0.17	0.0082	2.80	525 (7.4)

[a] At a platinum electrode. [b] $k^{\circ\prime}$ = 0.028 cm/s at a graphite electrode.

Table III. Potentials and Heterogeneous Rate Constants for the Complex of B in Aqueous Media in the Presence of Halide Ions[a]

medium	$E^{\circ\prime}(3\rightarrow2)$, V vs. SCE	k°, cm/s
0.1 N HNO_3/2 M KNO_3	0.08	0.14
0.1 N HNO_3/2 M KNO_3/0.01 M NaI	0.08	0.058
0.1 N HNO_3/2 M KNO_3/0.05 M NaI	0.08	0.024
0.1 N HNO_3/2 M KNO_3/0.1 M NaI	0.08	0.0056
0.1 N HCl/2 M KCl	0.02	0.13
0.1 N HCl/2 M KCl/0.05 M NaI	0.02	0.13
0.1 N H_2SO_4/0.5 M Na_2SO_4	−0.072	0.012
0.1 N H_2SO_4/0.5 M Na_2SO_4/0.1 M KCl	−0.066	0.013
0.1 N H_2SO_4/0.5 M Na_2SO_4/1.0 M KCl	−0.033	0.088
0.1 N H_2SO_4/satd Na_2SO_4/2 M KCl	−0.021	0.13
1 M 1:1 acetic acid	−0.068	0.024
1 M 1:1 acetic acid/2 M KCl	−0.064	0.052
1 M 1:1 adipic acid	−0.15	0.010
1 M 1:1 adipic acid/1 M KCl	−0.15	0.010

[a] Measured at room temperature and at a platinum electrode.

Table IV. Formal Potentials and Spectrophotometric Data of FeB^{2+} in Aqueous Media[a]

medium	pH	$E^{\circ\prime}(2\rightarrow3)$, V vs. SCE	λ_{max}, nm (ϵ_{max}, M^{-1} cm^{-1})
0.01 M HCl	2.3	0.12	630 (800)
0.01 M HCl (adjusted with NaOH)	7.0	0.12	630 (800)
1 M 1:1 cyanoacetic acid/ cyanoacetate buffer	2.45	−0.020	630 (800)
1 M 1:1 acetic acid/ acetate buffer	4.74	−0.10	630 (800)
0.5 M Na_2SO_4/5 mM NaOH	11.3	−0.56	630 (800)
0.01 M NaOH			630 (800)
0.1 M NaOH	12.9	−0.71	630, 725
1 M NaOH	14.0	−0.79	630, 725
4 M NaOH	14.6	−0.83	630, 725

[a] Iron(II) complexes of ligand B were electrogenerated in acidic aqueous solution and were either electrogenerated or chemically reduced in basic solutions from the iron(III) complex of ligand B.

with total buffer concentration, C (for 1–3 M solutions); the slope of the k_2' vs. C plot yielded a rate constant, k_2, of 2.1 × 10^{-3} M^{-1} s^{-1} at 25 °C. This is in excellent agreement with the value found from voltammetry measurements. Similar results were obtained with acetic acid/acetate buffered, unbuffered aqueous, and strongly acidic (HCl) solutions, which yielded k_2 values of 1.38 × 10^{-4}, 1.56 × 10^{-5}, and 1 × 10^{-2} M^{-1} s^{-1}, respectively (25 °C).

Solutions of FeB^{2+} produced by electroreduction of the 3+ species were deep blue and showed a λ_{max} of 630 nm and ϵ_{max} of 800 that was independent of the medium (Table IV). Although the FeB^{2+} species is stable on the cyclic voltammetric time scale in strongly acid media (see Figure 1), solutions of this species showed a slow decay of the peak at 630 nm. Plots of ln $(A - A_0)$ vs. t for several strong acid solutions are shown in Figure 11. The slopes are proportional to the strong acid concentration and yield a rate constant for disappearance of FeB^{2+} of 2.4 × 10^{-3} M^{-1} s^{-1} (25 °C). The increase in rate with proton concentration suggests that the rate-determining step in the dissociation reaction (2) may involve protonation of the complex. The 2+ complex is more stable in weakly acidic media. For example, in a 1 M 1:1 acetic acid/acetate buffer a 1 mM solution of FeB^{2+} showed an absorbance change of about 0.1 unit (from A = 0.8 at 630 nm) after 2 months. After about 6 months the absorbance had decayed to 0.4 and, thereafter, remained constant at this value. The FeB^{2+} species showed the same λ_{max} and ϵ_{max} and was quite stable in 0.5 M Na_2SO_4 solutions adjusted to pH 11.3. However, in more strongly basic solutions (pH <12.9) a new absorption at 725 nm grows in.

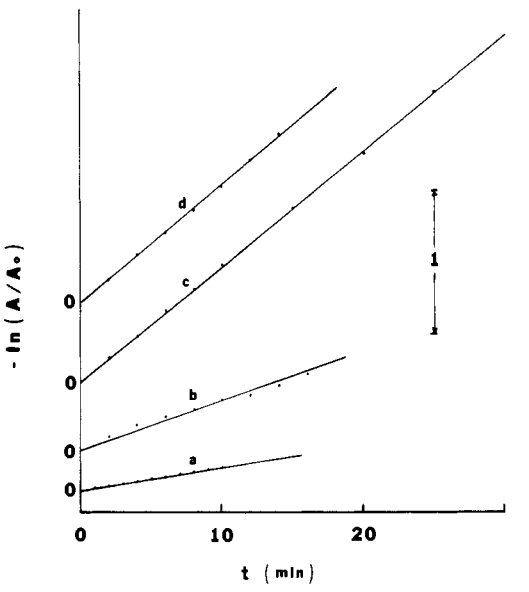

Figure 11. Change in absorbance with time for a 1 mM FeB^{2+} solution (electrogenerated from FeB^{3+}) in (a) 0.05 M H_2SO_4, (b) 0.25 M HCl, (c) 0.5 M H_2SO_4, and (d) 1 M CF_3COOH (A_0 is the initial absorbance; λ_{max} = 630 nm).

Discussion

The predominant species in the Fe–B system as a function of pH can be assigned, on the basis of voltammetric and spectrophotometric measurements and the variation of redox potentials with pH (Table I). These lead to the results shown in Figure 8. In acidic solutions the $FeB^{3+/2+}$ couple exists and yields a wave at −0.08 V vs. SCE independent of pH (line a). The large shift in $E^{\circ\prime}$ for this redox reaction compared with that of the uncomplexed $Fe^{3+/2+}$ species (+0.53 V vs. SCE) shows that the stability constant of iron(III) with B is larger than that of iron(II) by a factor of about 10^{10}. As shown in Table II, the formal potential for the $FeB^{3+/2}$ couple depends upon the medium. This probably results from ion pairing

between FeB^{3+} and FeB^{2+} and the different anions, which might also account for the variation of the diffusion coefficient, D_0, in the different media. Note that D_0 is smaller in buffers of diprotic acids (at pHs where appreciable concentrations of dianion are present) than in the presence of monoanions. The heterogeneous rate constant for electron transfer, k^0, is also affected by the anions present in the medium (Tables II and III). While this may be partly ascribed to ion-pairing effects, specific interaction of the anions with the platinum electrode surface may also play a role. This is almost certainly the case for the results with iodide ion, which is known to be strongly adsorbed on a Pt surface.[15,16] In slightly basic solutions, the wave shifts toward more negative values (line b) at −0.06 V/pH unit. This suggests addition of hydroxide ion to the FeB^{3+} species as an axial ligand with the redox reaction of line b corresponding to

$$FeB(OH)^{2+} + e^- \rightarrow FeB^{2+} + OH^- \quad (5)$$

From the usual means of analysis of potential–pH diagrams,[14] we estimate $E^{\circ\prime}$ for this half-reaction as −0.48 V vs. SCE (pH 14) and the equilibrium constant of reaction 6 as $K_a = 6.3 \times 10^{-8}$.

$$(FeB)_2O^{4+} + H_2O \rightleftharpoons FeBOH^{2+} + H^+ \quad (6)$$

The second voltammetric waves and those found in more basic solutions have been ascribed to reactions of the binuclear species. Line c of Figure 8 corresponds to reaction 7 with an

$$(FeB)_2O^{4+} + e^- \rightleftarrows (FeB)_2O^{3+} \quad (7)$$

$E^{\circ\prime} = -0.54$ V vs. SCE. The deviation of the line from the expected pH independence in the less basic region (curve e) probably arises from the instability of the $(FeB)_2O^{4+}$ form in these solutions (see reaction 3), as discussed previously. The voltammetric curves at different pHs (Figure 7) suggest that both forms exist at equilibrium at pHs near 8, with the monomeric form favored in more acidic solutions (eq 3). The existence of both dimeric and monomeric species of the couple has also been demonstrated by magnetic moment measurements.[4]

At pHs above 11, the dimer redox wave shifts toward more negative potentials (line d, slope 0.12 V/pH unit; line f, slope 0.06 V/pH unit). The pH change that occurs upon dissolution of the iron(III) binuclear complex in 5 mM NaOH suggests loss of two protons; the subsequent coulometry showed $n_{app} = 2$ (i.e., reduction of both iron(III) centers). However, the decomposition reaction in strongly basic media to produce hydrous ferric oxide leads to some uncertainty in the values of potential obtained, and further studies are required to delineate the exact nature of the species under these conditions.

Conclusions

The results of this investigation indicate these complexes are promising materials for redox batteries and photoelectrochemical cells. They are highly soluble ($FeBSO_4$, 4 M; $FeB(OH)SO_4$, 2 M in H_2O at room temperature),[12] and both forms are stable for solutions in the range $5 < pH < 11$ upon repeated cycling between the iron(III) and iron(II) forms. For example, a 1 M 1:1 acetic acid/acetate buffer could be cycled coulometrically in exhaustive electrolyses of 1-h duration at least 22 times without apparent loss of species.[12] Application of these compounds to photoelectrochemical cells (0.5 M Na_2SO_4) at p-WSe_2 electrodes has also been reported.[17]

Acknowledgment. This work was supported in its early stages by a grant from Texas Instruments under TI/DOE cooperative agreement DE-FC01-79ER 10,000 and later by the Solar Energy Research Institute. The advice and suggestions of Dr. K. S. V. Santhanam are gratefully acknowledged.

Registry No. FeB^{3+}, 90269-23-1; FeB^{2+}, 59451-77-3; $(FeB)_2O(ClO_4)_4$, 71882-22-9; $FeB(OH)(ClO_4)_2$, 13963-71-8; $(FeB)_2O^{3+}$, 71882-21-8; HNO_3, 7697-37-2; KNO_3, 7757-79-1; NaI, 7681-82-5; HCl, 7647-01-0; KCl, 7447-40-7; H_2SO_4, 7664-93-9; Na_2SO_4, 7757-82-6; NaOH, 1310-73-2; cyanoacetic acid, 372-09-8; trifluoroacetic acid, 76-05-1; acetic acid, 64-19-7; adipic acid, 124-04-9; tartaric acid, 87-69-4; propionic acid, 79-09-4; malonic acid, 141-82-2; succinic acid, 110-15-6.

(15) Balashova, N. A.; Kazarinov, V. E. In "Electroanalytical Chemistry"; Bard, A. J., Ed.; Marcel Dekker: New York, 1969; Vol. III.
(16) Lane, R. F.; Hubbard, A. T. *J. Phys. Chem.* **1975**, *79*, 808.
(17) Abruna, H. D.; Bard, A. J. *J. Electrochem. Soc.* **1982**, *129*, 673.

Contribution from the Departments of Chemistry, Mount Union College, Alliance, Ohio 44601, and Kent State University, Kent, Ohio 44242

Electron Transfer. 69. Mediation by Phenylglyoxylate[1]

W. FAYE HOLLAWAY, VANGALUR S. SRINIVASAN,[2] and EDWIN S. GOULD*

Received September 19, 1983

Both the monomeric phenylglyoxylato derivative of $(NH_3)_5Co^{III}$ (II) and the dimeric bridged $(Co^{III})_2$ complex (III) are reduced by Cr^{2+} via the chemical or radical-cation mechanism. Strongly absorbing Cr(III)-bound radical intermediates are observed in both instances. Internal electron transfer to Co(III) in the monomeric system proceeds at a specific rate of 93 s^{-1} and that in the dimeric system at 4.0 s^{-1} (25 °C, 1 M $HClO_4$). Reaction of the phenylglyoxylato derivative of $(H_2O)_5Cr^{III}$ (VII) with Cr^{2+} leads to yet another strongly absorbing (green) species having an association constant of 4.6×10^3 M^{-1}. Here, it appears that the incoming Cr^{2+} ion has become attached to the keto group of the ligand, with the "extra" electron delocalized over the two chromium centers and the ligand (VIII). This novel green pigment is reduced by excess Cr^{2+} to a highly charged polymeric Cr(III) derivative of the corresponding α-hydroxy acid. In the absence of excess Cr^{2+}, the pigment decays at nearly a constant rate. The latter decay appears to be related to release of phenylglyoxylic acid by aquation of its $(H_2O)_5Cr^{III}$ complex. A proposed mechanism for this bleaching, which results in a net 2e reduction of the ligand, features action of the keto acid as a reversible Cr(II) carrier that catalyzes disproportionation of the radical cation to the parent keto acid complex and the polynuclear hydroxy acid complex (IX).

Operation of the inner-sphere or bridge mechanism for electron transfer between metal centers was demonstrated in 1953.[3] Two years later it was shown that organic ligands could function as redox bridges.[4] Of the several mechanistic variations that have been characterized during the intervening

* To whom correspondence should be addressed at Kent State University.

(1) Sponsorship of this work by the donors of the Petroleum Research Fund, administered by the American Chemical Society, is gratefully acknowledged.

0020-1669/84/1323-2181$01.50/0